Journal of Environmental Management 373 (2025) 123536

Contents lists available at ScienceDirect

Journal of Environmental Management

journal homepage: www.elsevier.com/locate/jenvman

Research article

# CFD study on the effect of the baffles geometry in sedimentation efficiency in wastewater treatments through Large Eddy Simulations

P. Bruno [a], F. Bruno [a], G. Di Bella [a], E. Napoli [b], M. De Marchis [b,*]

[a] *University of Enna Kore, Cittadella universitaria, Enna, 94100, Italy*

[b] *University of Palermo, , Department of Engineering, Palermo, 90128, Italy*

ARTICLE INFO

*Keywords:*
Sedimentation
Computational Fluid Dynamics (CFD)
Large Eddy Simulation (LES)
Baffle design
Inlet flow

ABSTRACT

Sedimentation tanks represent one of the most important components of any water and wastewater treatment plants. The lack of knowledge of hydraulics in sedimentation tank leads to unnecessary capital and operating costs as well as water pollution in the form of excessive sludge. Improper and inadequate design cause overloading of filters, and lead to frequent backwashing, which in turn waste a significant percentage of treated water. Sedimentation tanks require a uniform flow field to ensure the correct operating conditions. Unfortunately, the development of circulation zones causes deep deviation from the uniformity, bringing negative effects on the efficiency of the tank. The focus of this study is to apply Computational Fluid Dynamics (CFD) to study and to improve the sedimentation efficiency through the optimization of the hydrodynamics inside settling tanks. In the present analysis, Large Eddy Simulation (LES) is used to simulate three-dimensional turbulent flow and scalar tracer transport in different settlers using a structured finite-volume discretization. The results show how the baffles' geometry, as well as the inlet design, influences the retention time distribution of the tank, varying the sedimentation efficiency. In particular, the increase of baffles inside the tank reduces the free space and allows a more uniform distribution of velocity vectors. This reduces both short circuits and recirculation zones bringing the flow closer to the ideal condition. On the other hand, the inlet position influences the velocity on the tank's bottom, with possible particles re-suspension effects.

## 1. Introduction

Sedimentation is a treatment process in which suspended particles, like flocs, sand and/or clay are removed from the water. Sedimentation is a natural process, clearly induced by gravity and affected by the flow field within the tanks. Water, in fact, moves inside the settlers through the length of the tank with a low speed giving the effluent enough time for sedimentation of solid particles. Sedimentation tanks can be rectangular with horizontal flow or circular with an up-flow pattern. In rectangular tanks, influent enters the basin at the inlet and energy dissipation is the main objective in designing a primary clarified inlet. Recently, Su et al. (2019) focused the attention on the influent flow rate variation on secondary flow, applying numerical techniques. The authors observed how energy of influent must be dissipated at the inlet zone by selecting the best position and configuration of inlet or using the baffles in the inlet zone (Krebs et al., 1995). In primary settling tanks, influent concentration is rather low and particles have minor influence on the flow field. Therefore, in the primary sedimentation tank, the buoyancy effects can be neglected (Rostami et al., 2011) and sedimentation performance mainly depends on the flow field characteristics in the tank. Otherwise, in the secondary (or final) sedimentation tank, the particles' concentration in influent is high and this involves a different decantation mechanism. One of the former study on the effect of baffle in water treatment is given by Ahmed et al. (1996) who performed experimental analysis focused on the determination of the optimal location and contraction of sedimentation tank baffles. Experiments were later performed by Asgharzadeh et al. (2011) aimed at found the effects of baffle configurations on the performance of a secondary sedimentation tank.

This work deals on the study of the flow inside primary sedimentation tanks. Here the sedimentation is considerably influenced by the hydrodynamic condition in the tank, so the literature studies focused the attention on determining the ideal geometric characteristics for an optimal sedimentation. A uniform flow field would be necessary for the efficient performance of a primary settling tank as this would allow particles to settle at a constant rate and over a short time. Unfortunately, the flow field in sedimentation tanks is turbulent, and such turbulence affects particle concentration and deposition; thus, if the turbulence is not correctly predicted, it may cause particles re-suspension reducing the sedimentation efficiency (Shahrokhi et al., 2012). Settler geometric

* Corresponding author.
*E-mail address:* mauro.demarchis@unipa.it (M. De Marchis).

https://doi.org/10.1016/j.jenvman.2024.123536
Received 28 June 2024; Received in revised form 12 November 2024; Accepted 28 November 2024

configuration often causes the development of areas characterized by whirling motions where the speed decreases or even vanish. These regions, also known as "dead zones", occupy a considerable volume of sedimentation tanks and, in this way, the effective volume for sedimentation process decreases and the suspended particles do not have sufficient space for deposition. The existence of the large circulation regions or dead zones in the settling tanks creates high flow mixing problems and causes the particle sedimentation decrease. In addition, these circulation zones reduce the effective volume of the tanks resulting in a short circuit condition between the inlet and outlet of the tank. Recently, Bruno et al. (2021) pointed out the role of recirculation region percentage on disinfection tanks, showing how water treatment efficiency increases when region occupied by large eddy is reduced. On the other hands, when almost of the domain is interested by large recirculation regions, water flow may leave the tank without any settling process (Shahrokhi et al., 2013). One applicable method to reduce the volume of the dead zones, increasing the performance of the sedimentation tanks is to use a proper baffle configuration (see Tamayol et al., 2010; Razmi et al., 2009 and literature therein cited). Other studies have found a relationship between the inlet deflector submergence and inlet eddy length, showing how larger vortices occur with smaller inlet openings, thus reducing the removal efficiency (see among others Imam et al., 1983). Recently, Computational Fluid Dynamics (CFD) was more and more applied to analyse elements of Water Treatment Plants, due to the ability of a numerical approach to achieve precise, fast and economic results with respect to the conventional experimental methods. As pointed out by Samstag et al. (2016) Computational fluid dynamics (CFD) is a rapidly emerging field in wastewater treatment (WWT), with application to almost all unit processes. The level of CFD's capability varies between different process units, with major application in the areas of final sedimentation, activated sludge basin modelling and disinfection, and greater needs in primary sedimentation and anaerobic digestion. CFD tools were also implemented as an adjuvant for physical model testing and for operation/maintenance guidance (see among others Li and Sansalone, 2020, 2021a and literature therein cited). CFD simulations were also used to develop new Machine Learning (ML) models able to improve regulation and geometric design of water treatment tanks and/or basin clarifications (Li and Sansalone, 2022b,a; Li et al., 2024). While clarification basins was implemented by regulatory stakeholders as part of urban/suburban land development, the elucidation of the transport/fate processes within basins as driven by basin hydrodynamics remains limited and challenging, even though the use of CFD to optimize hydrodynamics is clearly aligned with current trends towards digital water models in environmental management, and the sedimentation is still the major technology used in Waste Water Treatment Plants (WWTP). In this framework, Li et al. (2021b), Li and Sansalone (2021b), focused the attention on the impacts of permeable baffle retrofits on the response of an existing clarification basin in a continuous time domain. The authors observed how the elution behaviour of the basin as a system is controlled by hydrodynamics, which is modified and managed by the retrofit design and baffle details. Baffling improves volumetric utilization, delays the elution process, increases the residence time, and improves the particulate matter separation. Numerous studies showed that the transverse baffles inside settlers decrease short-circuiting affecting the velocity and concentration fields both in rectangular and in circular clarifiers (Wills and Davis, 1964; Bretscher et al., 1992). Numerical models revealed the importance of baffles in dissipating the kinetic energy of the incoming flow and reducing short-circuiting and indicated that the location of the baffle has a pronounced effect on the nature of the flow, greatly influencing the overall percentage of solids removal efficiency (Zhou et al., 1992; Huggins et al., 2004). Recent literature studies (Goula et al., 2008; Gao and Stenstrom, 2019; Bruno et al., 2024a; Tamayol et al., 2008) focused the attention on the effect of inlet baffle heights on flow patterns and particle trajectories throughout the tanks and found how baffle affects the inlet section.

The main objective of the present work is to investigate on the effects of the number and depth of baffles and of the inlet position on the performance of sedimentation tanks. Numerical simulations were carried out through Large Eddy Simulation (LES) technique. In many studies, Reynolds Averaged Navier–Stokes (RANS) based turbulence models were used with significant time savings, as they require lower computational costs. Even though RANS simulations are able to predict the mean flow in turbulent flows (see De Marchis and Napoli, 2008; de Marchis et al., 2012), it was demonstrated that they are not able to predict smaller scale eddies. These recirculation zones could be better simulated with Large Eddy Simulation (LES) models capable of accurately assessing the variation of turbulent fluctuations (see Bruno et al., 2024b; De Marchis et al., 2019). Furthermore, as pointed out by Li et al. (2021a), the instantaneous flow fields obtained in the LES provide insight into the underlying turbulent flow processes that are not available in a steady RANS approach. More recently, Li and Sansalone (2021a) performed a predictive capabilities of various RANS models based on the computed LES results as a benchmark. The comparisons of the RANS models with respect to LES and physical model measurements pointed out how LES model shows consistent and accurate performance over three different clarification system configurations, whereas the predictive capability of RANS models varied with respect to the specific geometries, suggesting the use of LES techniques. Similar consideration have been make by Al-Sammarraee et al. (2009), who simulated particle sedimentation in a longitudinal sedimentation basin using Large-eddy simulations. The authors observed a great deal of interactions with the sedimentation tank geometry which has significant improvements on the design aspects. The organization of the paper is as follow: Section 2 describes the numerical code adopted for LES and the computational domain is presented; in Section 3 results are presented and discussed whereas conclusions are drawn in Section 4.

## 2. Numerical approach

In the study of treatment plants, the application of numerical techniques allows to reduce the design times and to choose the optimal hydrodynamic configuration. Nowadays this is a fundamental point for the scientific community that works in these areas since it would help engineers in improving facility designs and consequently bring economic benefits before construction.

### 2.1. Governing equation of fluid flow

Turbulent flows, as previously mentioned, are resolved using LES approach, based on the numerical solution of the filtered continuity and momentum equations, given by:

$$\frac{\partial \overline{u}_i}{\partial t} + \frac{\partial \overline{u}_i \overline{u}_j}{\partial x_j} - \nu \frac{\partial^2 \overline{u}_i}{\partial x_j \partial x_j} + \frac{1}{\rho}\frac{\partial \overline{p}}{\partial x_i} + f_i = 0 \quad (1)$$

$$\frac{\partial \overline{u}_i}{\partial x_i} = 0 \quad (2)$$

where $u_i$ and $x_i$ are velocity and position in the $i$th direction, $t$ is time, $\rho$ is fluid density, $p$ is pressure, $\nu$ is the kinematic viscosity, and $f_i$ represents the force per unit of mass in the $i$th direction. The symbol $\overline{\cdot}$ indicate filtered quantities. The governing equations are resolved using the second-order accurate numerical model OpenFOAM (Open source Field Operations and Manipulations). Specifically, the transient solver pimpleFoam was applied to analyse the turbulent flow field and sediment transport for incompressible and Newtonian fluids. This solver is a combination of PISO (pressure-implicit split operator) and SIMPLE (semi-implicit method for pressure-linked equations) solvers. The PIMPLE algorithm is composed of an implicit momentum predictor and several pressure–velocity correctors. In the PIMPLE loop, the velocity equations are firstly solved by using the velocity and pressure fields of the previous time step, known as momentum predictor. The velocity and pressure are corrected several times afterwards to satisfy mass conservation. Here LES techniques are preferred due to their ability in predicting the properties of specific turbulent flows and providing flow details which can be used like data to test and refine other turbulence-closure models. LES focuses on larger eddies (whirls of fluid) in a flow, influenced by the geometry of the flow, while the smaller, more universal scales are modelled using a subgrid-scale (SGS) model. This methodology stems from Kolmogorov's theory of self-similarity, which suggests that larger eddies are shaped by flow geometry, whereas smaller scales are more universal. Different LES subgrid models are available for incompressible flows. In this case, Wall-Adapting Local Eddy-Viscosity (WALE) model was used, where the eddy viscosity is modelled by:

$$\nu_t = \rho L_s^2 \frac{(S_{ij}^d S_{ij}^d)^{(3/2)}}{(\overline{S}_{ij}\overline{S}_{ij})^{5/2} + (S_{ij}^d S_{ij}^d)^{(5/4)}} \tag{3}$$

where $\nu_t$ is the subgrid-scale turbulent viscosity, $L_s$ is the mixing length for subgrid scales, $\overline{S}_{ij}$ is the rate-of-strain tensor for the resolved scale defined by:

$$\overline{S}_{ij} = \frac{1}{2}\left(\frac{\partial \overline{u}_i}{\partial x_j} + \frac{\partial \overline{u}_j}{\partial x_i}\right) \tag{4}$$

In the WALE model $L_s$ and $S_{ij}^d$ are respectively defined as:

$$L_s = min(k \cdot d, C_w V^{(1/3)}) \tag{5}$$

where k is the von Kármán constant, d is the distance to the closest wall, $C_w$ is the WALE constant equal to 0.325 and V is the volume of the computational cell and $S_{ij}^d$ is given by:

$$S_{ij}^d = \frac{1}{2}(\overline{g}_{ij}^2 \overline{g}_{ij}^2) - \frac{1}{3}\delta_{ij}\overline{g}_{kk}^2 \tag{6}$$

with $\overline{g}_{ij} = \frac{\partial \overline{u}_i}{\partial x_j}$. Details of the numerical code can be found in the wiki documentation reported in specific website www.openfoam.com. The numerical model has been previously validated in WWTP by Bruno et al. (2020, 2021), where the disinfection tank efficiency was analysed through LES techniques and the results perfectly agree with experimental data.

### 2.2. Governing equation of tracer transport

The hydraulic efficiency of settling tanks is evaluated considering the flow of a non-reactive tracer injected inside the tank to obtain the mean residence time. In CFD simulations two main methods can be used to investigate on contaminant/sediment dispersion in water treatment. The first method is to simulate the particles tracking in a Lagrangian way (De Marchis et al., 2017; De Marchis and Milici, 2016; Milici et al., 2020; Milici and De Marchis, 2016; Milici et al., 2020; Saccone et al., 2023), the second one is to simulate tracers in Eulerian way (Li et al., 2021a,b; Demirel and Aral, 2016). A passive scalar is a conservative substance that is transported along the volume of fluid without interfering with local hydrodynamics (Fraga, 2017). A recent model, known as interAdsFoam, was developed by Li and Sansalone (2022c) for multiphase and multiphysics Computational Fluid Dynamics. The model can be used to simulate turbulence mixing and adsorption with dynamic water–air interface and reaction zones. In the proposed research, the hydrodynamic within the tanks was analysed through the application of the OpenFOAM model for passive scalare in sedimentation processes. Basically, tracer studies are performed by inserting the tracer at the inlet and measuring the response at the outlet in order to obtain residence time statistics (see, Zhang et al., 2014). The tracer is modelled as a passive scalar. In this specific case, the tracer is injected with a uniform distribution from the inlet for a time of 30 s and the outlet concentration variation is monitored throughout the numerical simulation. In order to simulate the transport of the conservative tracer, standard solver pimpleFoam is modified including the following advection–diffusion equation:

$$\frac{\partial \overline{C}}{\partial t} + \overline{u}_j \frac{\partial \overline{C}}{\partial x_j} = \frac{\partial}{\partial x_j}\left((D + D_t)\frac{\partial \overline{C}}{\partial x_j}\right) \tag{7}$$

where $\overline{u}_j$ is the velocity component along the j-direction (i.e. x, $y$ and z), t is the time, $x_i$ and $x_j$ represent the Cartesian coordinates, $\overline{C}$ is the filtered tracer concentration, D is molecular diffusivity, which is negligible compared to turbulent diffusivity $D_t$. The turbulent diffusivity can be computed as $D_t = \nu_t / Sc$ where $\nu_t$ is eddy viscosity calculated in Eq. (3), while Sc is the turbulent Schmidt number which is set to 1000 (Donzis et al., 2014). Here a simplified condition is simulated where the sedimentation Type II induced by flocculated particles is neglected.

### 2.3. Flow domain, simulation setup and boundary conditions

Fig. 1 shows the settler model used in the present study to simulate flow and tracer transport in sedimentation treatments. The tank simulates sedimentation process inside a full-size tank with a longitudinal length of 11.20 m, a width of 2.00 m and an overall height of 4.50. The Inlet is 40 cm high, while the baffle located in the immediate vicinity of the inlet extends 60 cm below the free surface, leaving a 40 cm high space for the passage of the flow. A 1.50 × 1.50 m hopper positioned below the inlet allows the accumulation of precipitated sludge. The water enters the settler with a constant discharge of 0.24 $m^3/s$ from the inlet located at the left of the tank and flows towards the outlet section located on the opposite side. The computational domain was decomposed through a Cartesian grid (Fig. 2) using 354 × 120 × 120 cells in the streamwise, spanwise and wall-normal directions respectively, for a total of 5,097,600 cells. The cells size was determined following a sensitivity analysis, establishing a greater refinement of the grid near the walls and baffle walls in order to resolve steep velocity gradients and to capture the peak of the Residence Time Distribution (RTD) of the tracer. Four different mesh were compared and it was observed a peak underestimation for coarse mesh resolution. Specific attention was done for the proper boundary conditions imposition. As customary, the effects of roughness on the walls was neglected, while zeroGradient and no-slip conditions was imposed on the walls for pressure and velocity respectively. Specific boundary conditions were applied on the bottom and lateral walls, where zero-gradient condition is imposed (kqRWallFunction) for turbulence kinetic energy and Reynold stresses. On the walls, a specific wall constraint on the turbulent viscosity (nutkWallFunction) is imposed. The reader can refer to the OpenFOAM user guide for specifics about the model (see www.openfoam.com/documentation). Periodic boundary conditions were imposed in the streamwise direction for velocity. These boundary conditions make the results independent on the inlet turbulence intensity avoiding unwanted flow disturbances occurring when different boundary conditions are applied at the inlet and outlet (Kim et al., 2010). A uniform concentration was injected into the tank applying a fixedValue boundary condition for the tracer, in such a way that the scalar enters uniformly from the entire inlet cross section, while zeroGradient boundary condition was used at the outlet and walls. Symmetry boundary condition was finally imposed on the upper face of the domain since free-surface effects are negligible (Zhang et al., 2013; Kim et al., 2010). Numerical simulations were conducted using OpenFOAM code, which solves the governing equations through the finite volume method. For the temporal discretization of the governing equations, the second-order backward scheme is used. A constant time step was set to maintain the Courant–Friedrich–Levy (CFL) number below 0.5. LinearUpwind and Gauss linear schemes were used for the treatment of the convective and diffusive terms respectively, ensuring a second order accuracy of the numerical method. Initially, the flow inside the reactor was simulated without the tracer for a time of 300 s in order to allow the flow field stabilization, excluding the wake fluctuations

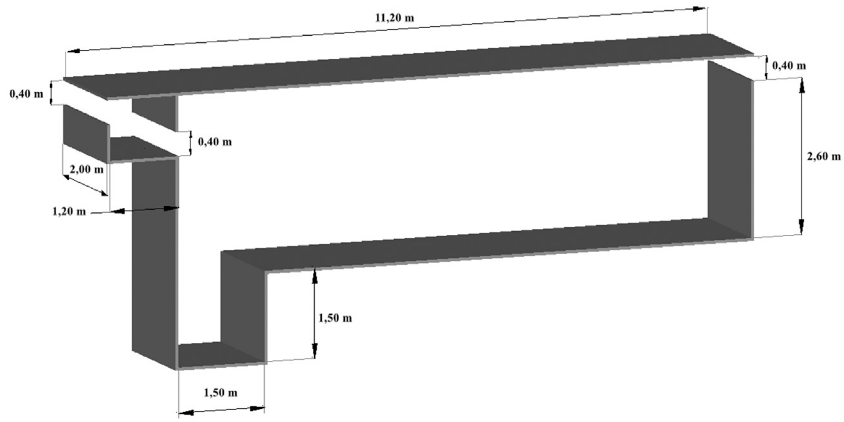


**Fig. 1.** Three-dimensional schematic view of the computational domain.

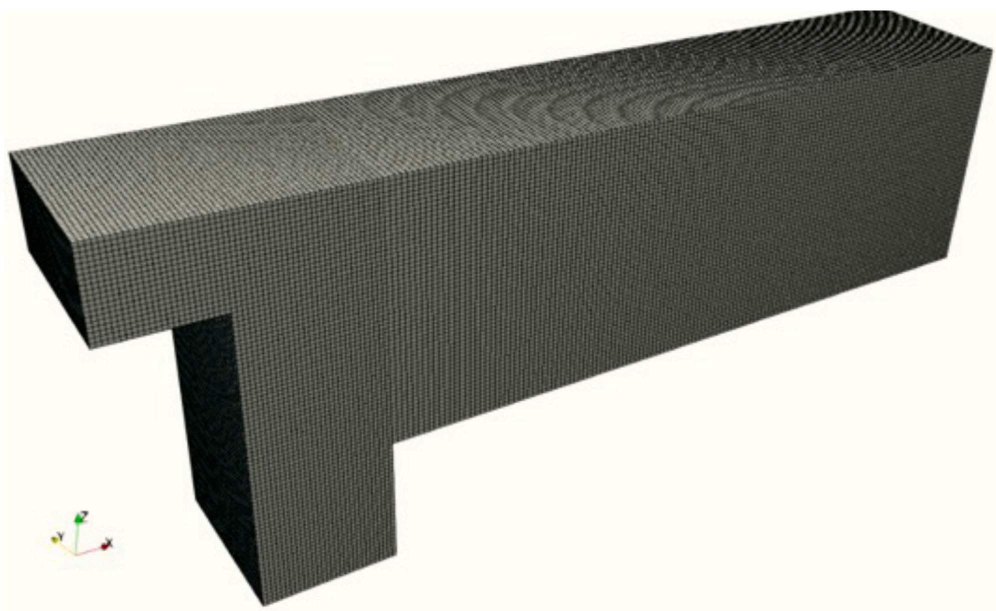

**Fig. 2.** Three-dimensional view of the structural mesh.

generally observed during the initial phases of a simulation (Demirel and Aral, 2016). Once the flow field was established, the tracer was released inside the tank for a period of 30 s and the simulation was run for an additional 1000 s thus to ensure that almost all the injected tracer passes through the outlet. In the following sections the different geometries are presented and discussed.

### 2.4. Geometrical configurations

Sedimentation performances strongly depends on the geometry of the tank and its hydrodynamic condition. Different geometries were designed allowing the flow to be brought closer to the ideal condition (plug flow case) and therefore optimizing the efficiency of the sedimentation process. In light of this, literature studies have shown that it is possible to reduce the development of short circuits and recirculation phenomena by inserting transverse baffles or varying the inlet position. In these previous studies a single geometrical configuration was analysed. The main objective of the present work is to investigate on the effects of two main geometric points: number of baffles, located in the streamwise direction, and depth of baffles in a systematic study able to give more insights to optimize sedimentation tanks. To this aim, in the proposed study, five sedimentation tanks, characterized by different number and geometry of baffles, were analysed. Basically, starting from the classical geometry without baffle, case $TC_0$ shown in Fig. 2, four additional geometries were considered adding a baffle for each configuration ($TC_1$-$TC_4$). These geometries were analysed in order to give insight on the effect of the baffle number on the sedimentation efficiency. In order to observe the effect of baffle depth, a second set of simulations was performed simulating other 4 different geometries. Specifically, we kept constant the number of baffles, equal to 4, and systematically increase the baffle depth ($TC_5$-$TC_8$). In this way, it is possible to gradually increase the mixing phenomena and investigate on effect of a more complex hydraulic pattern. In the second set of simulation the effect of the inlet location was also analysed. Table 1 reports details about the different cases of baffles and opening positions modelled in this study underling the number, the position from the inlet slot and the baffles length. The d/L value indicates the ratio between the distance of the baffle from the inlet (d) and the total length of the tank (L). As regards the opening position, two different configurations inlet positions were tested: near the surface and near the bottom. Sedimentation performances strongly depends on the geometry of the tank and its hydrodynamic condition and the difference simulated cases were chosen to reduce short circuits within the tank.

**Table 1**
Descriptions of different inlet and baffle cases.

| Case number | Inlet position | Baffles number | Baffles location (d/L) | | | | $H_b$ Baffle depth |
|---|---|---|---|---|---|---|---|
| | | | 1st $baffle$ | 2st $baffle$ | 3st $baffle$ | 4st $baffle$ | |
| $TC_0$ | surface | 0 | – | – | – | – | – |
| $TC_1$ | surface | 1 | 0.10 | – | – | – | 0.60 |
| $TC_2$ | surface | 2 | 0.10 | 0.75 | – | – | 0.60 |
| $TC_3$ | surface | 3 | 0.10 | 0.50 | 0.75 | – | 0.60 |
| $TC_4$ | surface | 4 | 0.10 | 0.25 | 0.50 | 0.75 | 0.60 |
| $TC_5$ | surface | 4 | 0.10 | 0.25 | 0.50 | 0.75 | 1.00 |
| $TC_6$ | bottom | 4 | 0.10 | 0.25 | 0.50 | 0.75 | 1.00 |
| $TC_7$ | bottom | 4 | 0.10 | 0.25 | 0.50 | 0.75 | 1.50 |
| $TC_8$ | bottom | 4 | 0.10 | 0.25 | 0.50 | 0.75 | 2.00 |

## 3. Results

The effect of different baffle arrangements in the sedimentation tank was compared using two methods: a qualitative method, comparing the size of the circulation zone and the velocity field; and through a quantitative method, estimating the FTCs (Flow Through Curves), which gives some information about short-circuiting, degree of mixing and hydraulic efficiency in the tanks. The proper position for the baffle is obtained when the volume of the circulation zone is minimized. Circulation zones may also induce high turbulence intensities in some regions. This condition not only reduces the possibility of particle deposition, but may also cause resuspension phenomena. Therefore, minimization of the circulation zone is essential to find the suitable location of the baffle and consequently improve sedimentation process. Starting from the conventional geometry with a single baffle near the inlet (d/L = 0.1), the effects due to the addition of a different number of baffles, having the same height ($H_b$ = 0.60 m), were evaluated. Fig. 3 plots the predicted streamlines for the different types of baffle configuration in the settling tanks and the contour of the mean velocity flow field in the central region of the domain. Specifically, in the left panels the streamlines are reported, whereas in the right panels streamwise velocity contour are depicted. The flow pattern is characterized by a large recirculation region occupying a large part of the tank from top to bottom.

Without baffles (Fig. 3(a)), a large circulation zone exists in the whole region just below the surface of the settling tank, which approximately occupies 70% of the total volume of the tank. Moreover, looking at the contour plot (Fig. 3(f)) it is evident a main current directed towards the outlet near the free surface, whereas a wide negative region are visible at medium depth and close to the tank bottom. This kind of hydrodynamic clearly reduces the sedimentation process. In order to improve the sedimentation efficiency, vertical baffles were added near the free surface. Specifically, by inserting the conventional baffle (Fig. 3(b)) near the inlet, there is a reduction in the recirculation areas, even though the velocity contour reveals only a small deviation of the mean flow directed towards the outlet section. By increasing the number of baffles, positioned at the same height from the free surface but at a different distance from the inlet, a reduction in the size of the recirculation regions is observed. The shown velocity distributions suggest an improvement of the sedimentation efficiency increasing the number of baffles. Focusing the attention on the right panels of Fig. 3, it can be observed the effect of the baffle on the main velocity field. Specifically, increasing the baffle number the mean flow directed from the inlet towards the outlet disappears and a more complex hydrodynamic is developed in the tank. The mean velocity field is more and more evenly distributed along the tank's height. This means that the baffles inside the tank allows a more uniform and calm velocity conditions improving the settlement of the particles. In cases $TC_0$ and $TC_1$, plotted in Fig. 3-(f) and -(g), the area occupied by the negative x-velocity is too large and the excessively high-speed causes obvious short-circuits. Adding a baffle in the outlet region, case $TC_2$, the velocity profile is slightly more uniform, even though negative velocity areas are still considerable. In case $TC_3$, interestingly, a deviation of the velocity field is observed both near the bottom and near the inlet. The third baffle causes, in fact, a recirculating region near the free surface and near the hopper, inducing a channelling effect of the water inlet directed towards the bottom. This specific behaviour disappears in case $TC_4$ where a total of 4 baffles are simulated. The analysis of streamwise velocity field in case $TC_4$ reveals the developed of a different hydrodynamic, characterized by a more uniform positive velocity directed towards the outlet, with reduced velocity, and a small negative velocity close to the hopper. This kind of hydrodynamic suggests an improvement of the sedimentation efficiency.

In order to confirm the results above shown, a quantitative analysis is required. As previously mentioned, it is possible to evaluate the hydraulic efficiency of sedimentation tanks considering the flow of a passive scalar tracer injected from the inlet for a time of 30 s. The tracer distribution analysis is based on the examination of the RTD (Residence Time Distribution) curve obtained at the outlet. In Fig. 4 the RTD curves are depicted. Specifically, $\theta$ = t/$\tau$, the nondimensionalized time with respect to the theoretical mean residence time ($\tau$= V/Q) is plotted against the tracer normalized concentration, calculated according to:

$$E(\theta) = \frac{C}{\frac{C_{init} \cdot T_{realese}}{\tau}} \tag{8}$$

where $C_{init}$ = 1 is the uniform concentration of tracer injected at the inlet and $T_{release}$ = 30 s is the injection period, which is about 10% of theoretical detention time $\tau$. The results, shown in Fig. 4, are in agreement with the other recent researches (see among others Tamayol et al., 2008; Shahrokhi et al., 2012 and literature therein cited). More specifically, the peak of the normalized RTD graph obtained for the no baffle case ($TC_0$) indicates that high quantities of tracer leave the reactor after a shorter time than the theoretical hydraulic residence time $\tau$. Without baffles, in fact, most of the tracer leaves the tank in a normalized time t/$\tau$ equal to 0.2 and, for the remaining time the outlet concentrations are almost zero. This confirms that no baffle settlers suffer from short-circuit phenomena that reduce sedimentation efficiency. Substantially, highest peaks indicate low sedimentation efficiency. The current, as depicted in Fig. 3, is mainly directed towards the outlet section, flowing in the free surface region characterized by highest velocity. By inserting baffles inside the tank, the peak becomes much less pronounced and moves to the right since the reduction of circulation areas reduces the short-circuiting effects. In particular, the introduction of the fourth baffle ($TC_4$) allows the tracer to stay for a long time inside the tank by shifting the RTD peak to a normalized time of about 0.35. On the other hand, the peak dimensionless tracer concentration passes from a value of 5.37 without baffles $TC_0$ to a value of 2.65 in case with 4 baffles (Case $TC_4$). FCT method therefore confirms the results obtained from previous studies performed through numerical fluid dynamics in similar water treatment tank (Bruno et al., 2020, 2021; Tamayol et al., 2008; Shahrokhi et al., 2012).

The above shown results are confirmed by the cumulative normalized RTD plot, obtained by integrating the RTD curve:

$$F(\theta) = \int_0^\infty E(\theta) d\theta \tag{9}$$

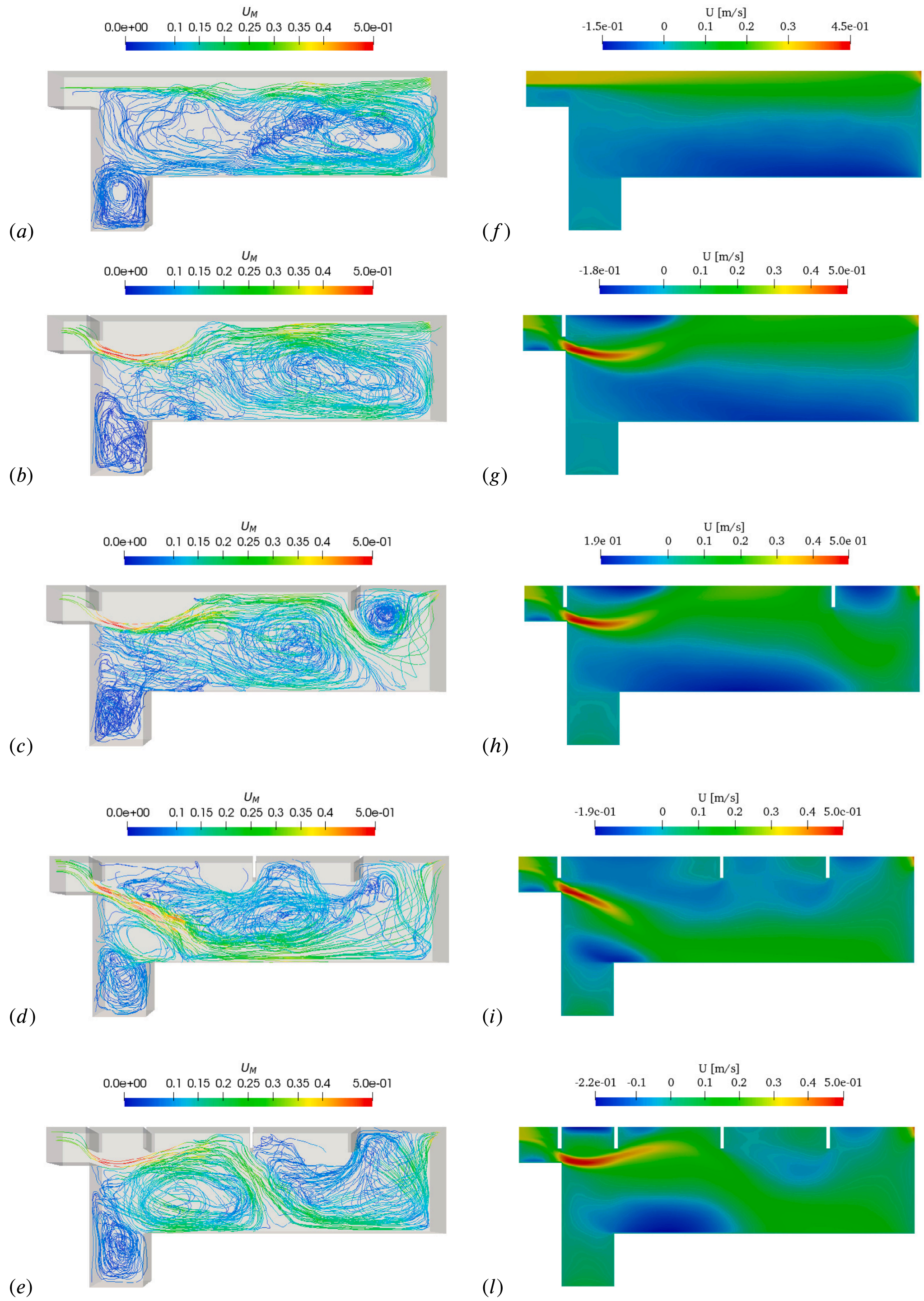


**Fig. 3.** Computed streamlines and velocity contour for baffle height (Hb = 0.60 m): (a)–(f) $TC_0$ no baffle; (b)–(g) $TC_1$ 1 baffle; (c)–(h) $TC_2$ 2 baffles case; (d)–(i) $TC_3$ 3 baffles case; (e)–(l) $TC_4$ 4 baffles case. Left panels: streamlines coloured with the velocity module $U_M$ (m/s); right panels: contour of the streamwise velocity field U (m/s). (For interpretation of the references to colour in this figure legend, the reader is referred to the web version of this article.)

In Fig. 5 the Cumulative RTD is depicted. The curves confirm the results shown in Fig. 4. Increasing the baffle number the cumulative RTD is shifted towards the ideal condition achieved for $\theta = 1$. Specifically, the introduction of the fourth baffle (case $TC_4$) gives rise to the best result.

From the cumulative RTD plot, it is possible to determine the indices usually applied to evaluate the hydraulic and mixing efficiencies of sedimentation tanks (see Bruno et al., 2020, 2021). Table 2 shows the comparison between the Hydraulic Efficiency Indicators (HEI) considered in the present study for the different cases. $t_{10}/\tau$, $t_{25}/\tau$, $t_{50}/\tau$, $t_{75}/\tau$ and $t_{90}/\tau$ represent the normalized times, starting from the introduction of the tracer, respectively necessary for the passage through the outlet of 10%, 25%, 50%, 75% and 90% of the mass of the tracer injected. The first index $t_0/\tau$ represents the normalized instant in which the tracer arrives at the outlet for the first time. $t_{max}/\tau$ is the time when the concentration at the outlet is maximum. More specifically, high $t_0$ and $t_{10}$ values indicate a reduced short-circuiting probability; high values of $t_{75} - t_{25}$ and $t_{90} - t_{10}$ and $t_{90}/t_{10}$ parameters indicate high level of velocity mixing in the tank. Meanwhile, $t_{50}$ and $t_{max}$ are parameters for predicting the efficiency of the tank. The higher values of these parameters lead to higher performance. The HEI values here

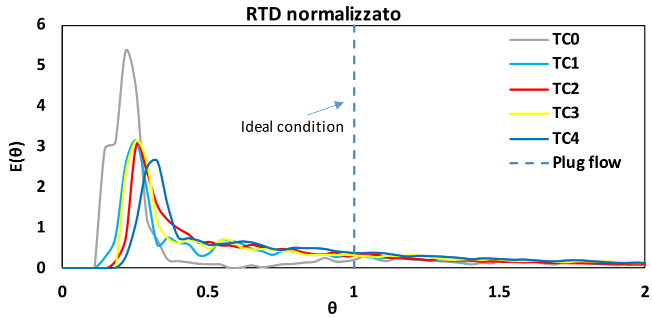


**Fig. 4.** Normalized RTD diagram obtained for no baffle $TC_0$ and $TC_1$, 1 baffle case; $TC_2$, 2 baffles case; $TC_3$, 3 baffles case; $TC_4$, 4 baffles case.

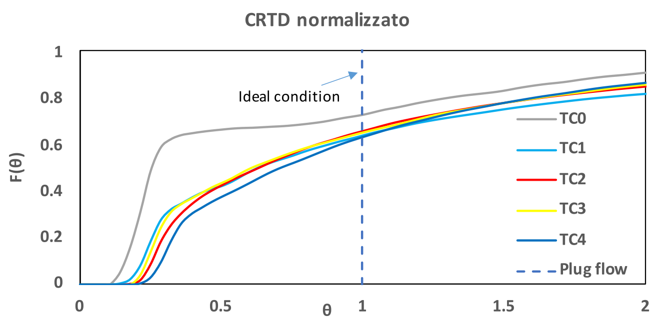


**Fig. 5.** Cumulative normalized RTD diagram obtained for no baffle $TC_0$ and $TC_1$, 1 baffle case; $TC_2$, 2 baffles case; $TC_3$, 3 baffles case; $TC_4$, 4 baffles case.

analysed show that in the no baffle case there is an evident short-circuit phenomenon since the values of $t_0$ and $t_{10}$ are extremely low. The insertion of a baffle near the inlet (case 1) allows the reduction of the short circuit highlighted by the increase in the value of $t_0$ and $t_{10}$, in accordance with the results obtained from the hydrodynamic study of the tank. The increase in the baffles' number allows a further shift of the curve to the right, and therefore an increase in the value of the HEI parameters is recorded, even if this increase is not substantial. With the configuration that the tracer study proved to be the best (four baffles), in fact, values of $t_0$ and $t_{10}$ are still far from the optimal condition ($t/\tau$ = 1). Either way, the most efficient configuration is achieved with 4 baffles, case ($TC_4$). This configuration, in fact, shows the highest $t_0$ and $t_{10}$ values, indicators of a low degree of short circuit, the lowest $t_{75}-t_{25}$, $t_{90}-t_{10}$, and $t_{90}/t_{10}$ values, indicators of high mixing efficiency, and the highest $t_{50}$ and $t_{max}$ values demonstrating high hydraulic performances.

Starting from the four baffles configuration, characterized by the best result in terms of hydraulic efficiency indicators, other geometries were investigated by increasing the depth of the baffles below the free surface of the tank and by changing the inlet position. Specifically, as reported in Table 1, cases $TC_5$, $TC_6$, $TC_7$ and $TC_8$ have the same number of baffles, equal to 4, but increasing depth $H_b$ from 0.6 to 2.00 m. In order to verify the effect of these new configurations, both qualitative and quantitative indicators were analysed. In Fig. 6 streamlines and streamwise velocity contours are depicted. Focusing the attention on the streamlines behaviour, left panels of Fig. 6, it can be observed how the height of the deflector $H_b$ does not involve substantial variations in the hydrodynamic condition of the tank since it does not allow the reduction of the areas occupied by recirculation. In addition, looking at the contour plots, is evident how increasing the height of the deflectors, an increase of the bottom velocity is observed with consequent disturbance of the calm condition, inducing re-suspension of particles that have already settled. The lowering of the inlet position has very similar consequences as it generates a preferential path at high speed in the bottom of the tank. The qualitative results are confirmed through the quantitative analysis depicted in Fig. 7, where the RTD curves for cases

**Table 2**
Descriptions of different inlet and baffle cases. Quantities are normalized with the theoretical mean residence time $\tau$ = V/Q.

| Case number | $t_0$ | $t_{10}$ | $t_{75}-t_{25}$ | $t_{90}-t_{10}$ | $t_{90}/t_{10}$ | $t_{50}$ | $t_{max}$ |
|---|---|---|---|---|---|---|---|
| $TC_0$ | 0.108 | 0.159 | 0.861 | 1.716 | 11.768 | 0.255 | 0.216 |
| $TC_1$ | 0.144 | 0.222 | 1.190 | 2.906 | 14.112 | 0.625 | 0.252 |
| $TC_2$ | 0.180 | 0.256 | 1.001 | 2.224 | 9.680 | 0.626 | 0.252 |
| $TC_3$ | 0.216 | 0.237 | 1.048 | 2.087 | 9.810 | 0.550 | 0.252 |
| $TC_4$ | 0.225 | 0.289 | 0.993 | 1.938 | 7.698 | 0.701 | 0.324 |

**Table 3**
Quantities are normalized with the theoretical mean residence time $\tau$ = V/Q.

| Case number | $t_0$ | $t_{10}$ | $t_{75}-t_{25}$ | $t_{90}-t_{10}$ | $t_{90}/t_{10}$ | $t_{50}$ | $t_{max}$ |
|---|---|---|---|---|---|---|---|
| $TC_4$ | 0.250 | 0.289 | 0.993 | 1.938 | 7.698 | 0.701 | 0.324 |
| $TC_5$ | 0.250 | 0.278 | 1.098 | 2.035 | 8.323 | 0.633 | 0.320 |
| $TC_6$ | 0.250 | 0.273 | 1.046 | 2.284 | 9.347 | 0.458 | 0.320 |
| $TC_7$ | 0.250 | 0.261 | 1.131 | 2.107 | 9.067 | 0.492 | 0.310 |
| $TC_8$ | 0.250 | 0.241 | 1.146 | 2.331 | 10.673 | 0.638 | 0.288 |

$TC_4$-$TC_8$ are plotted. Specifically, $\theta$ = t/$\tau$, the nondimensionalized time with respect to the theoretical mean residence time ($\tau$ = V/Q) is plotted against the tracer normalized concentration (see Eq. (8)). The RTD curves does not show a benefit induced by the baffle depth. All the cases are characterized by a very similar concentration profiles. The peak is almost the same in term of magnitude and normalized time. The best result is achieved for the $TC_4$ case, having a lowest peak. This result suggests that the optimal baffle depth can be identified in 0.60 m, below the free surface. The best baffle configuration can be better observed through the cumulative RTD plot, depicted in Fig. 8, where it is possible to observe a lower cumulative RTD for case $TC_4$. The results plotted in Fig. 8 are then used to estimate the Hydraulic Efficiency Indicators (HEI).

In order to give a quantitative analyse of the effect of dimension of the baffles, Table 3 reports the HEI values obtained for the four baffles configurations with different baffle height and inlet position. The time required to reach the outlet section, $t_0$ is practically identical for all the analysed cases; while the higher $t_{10}$ value was obtained for the configuration with the traditional position of the inlet (superficial) and with the height of the baffles equal to the minimum value of 0.60 m (case $TC_4$). Therefore, also in this case, FCT method confirms the results achieved for the first set of simulations; in case $TC_4$ there is less probability of short-circuiting. The values of $t_{75}-t_{25}$, $t_{90}-t_{10}$, and $t_{90}/t_{10}$ illustrate the degree of flow mixing and, again, are the lowest for case $TC_4$. Moreover, also the higher values of $t_{50}$ and $t_{max}$ demonstrate higher hydraulic performance. Therefore, case $TC_4$ has the best hydraulic efficiency and, for all the parameters analysed, is considered the best case in settling tanks here investigated. Further analysis are clearly required to find a configuration able to improve the sedimentation efficiency.

## 4. Conclusions

Sedimentation by gravity is one of the most common applied techniques in the removal of suspended solids from water and wastewater. The knowledge of the tank's hydrodynamics is important for a correct sizing in order to avoid the passage in suspension of the settled solids and their leakage with the clarified. In this study, LES turbulence approach is employed in order to accurately simulate and predict big and small recirculation zones in the tank. Tracer studies show that the conventional tank designs suffer from high short-circuiting and development of dead zones resulting in poor sedimentation efficiency. Furthermore, these phenomena do not allow the calm in the tank which is essential for solids' sedimentation. Here, the effects due to the insertion of baffle to modify the hydrodynamic flow field within the tank is investigated. Specifically, the number and the depth of the baffles, as well as the injection position of the flow were analysed. The

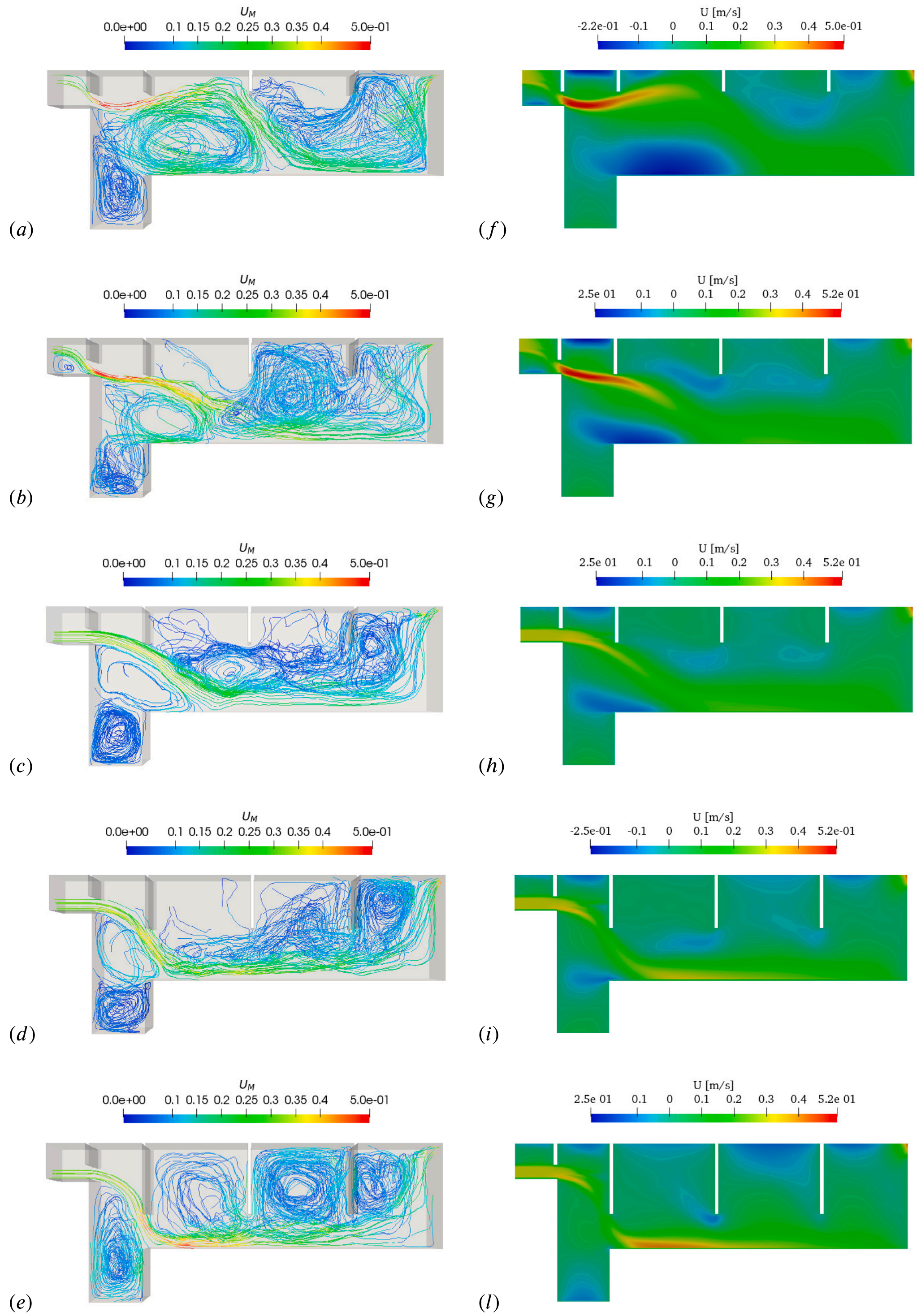


**Fig. 6.** Computed streamlines and velocity contour for baffle height (Hb = 0.60 m): (a)–(f) $TC_4$ 4 baffles $H_b$ = 0.6, upper inlet; (b)–(g) $TC_5$ 4 baffles $H_b$ = 1.0, upper inlet; (c)–(h) $TC_6$ 4 baffles $H_b$ = 1.0, bottom inlet; (d)–(i) $TC_7$ 4 baffles $H_b$ = 1.5, bottom inlet; (e)–(l) $TC_8$ 4 baffles $H_b$ = 2.0, bottom inlet. Left panels: streamlines coloured with the velocity module $U_M$ (m/s); right panels: contour of the streamwise velocity field U (m/s). (For interpretation of the references to colour in this figure legend, the reader is referred to the web version of this article.)

study was performed both using a qualitative and a quantitative point of view. Streamlines and flow field contours give a clear visualization of the hydrodynamics within the simulated tanks, showing the effect of the baffles on the recirculating flow and on the position of high and low speed regions. On the other hand, a quantitative analysis was given through the time index $t_{10}/\tau$, $t_{25}/\tau$, $t_{50}/\tau$, $t_{75}/\tau$ and $t_{90}/\tau$, the normalized times, starting from the introduction of the tracer, respectively necessary for the passage through the outlet of 10%, 25%, 50%, 75% and 90% of the mass of the tracer injected and time index. Specifically, the following results can be summarized:

- number of baffles in the tank; the sedimentation efficiency without baffle were compared with those achieved with 1 baffle, 2 baffles 3 baffles and 4 baffles. Overall, results show how the introduction of baffles improves tank efficiency in terms of sedimentation since the baffle acts as a barrier, effectively suppressing

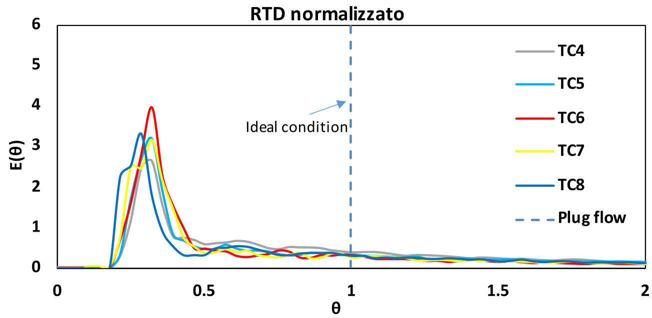


**Fig. 7.** Normalized RTD diagram obtained for $TC_4$, $TC_5$, $TC_6$, $TC_7$ and $TC_8$ baffles cases models.

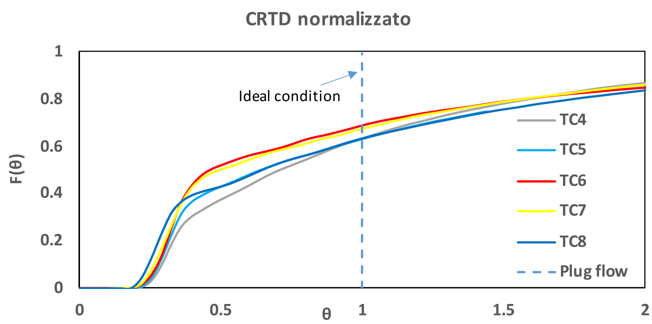


**Fig. 8.** Cumulative normalized RTD diagram obtained for $TC_4$, $TC_5$, $TC_6$, $TC_7$ and $TC_8$ baffles cases models.

the horizontal velocities of the flow and reducing the size of the dead zones. A baffle also reduces kinetic energy and induces a decrease in maximum magnitude of the streamwise velocity compared with the no-baffle tank. In particular, the configuration with four baffles with a conventional height (0.60 m) seems to be the optimal configuration. The velocity profile is, in fact, uniform enough for almost the entire length of the tank and the maximum velocity is far from the bottom, with advantages in terms of sedimentation efficiency;

- depth of the baffles; four different heights were simulated. The results pointed out how increasing the baffle depth does not give improvement in the sedimentation efficiency. Conversely, an increase in the bottom velocity is registered with consequent disturbance of the calm condition that cause re-suspension of particles that have already settled. It was found how a baffle depth of 0.60 m gives the optimal hydraulic efficiency;
- inlet position of the flow; two different injection points were simulated. The flow field as well as the RTD does not show quantitative modification of the efficiency of the tank. Only slight local modification of the hydrodynamic was observed.

## CRediT authorship contribution statement

**P. Bruno:** Writing – original draft. **F. Bruno:** Writing – original draft. **G. Di Bella:** Writing – original draft. **E. Napoli:** Writing – original draft. **M. De Marchis:** Writing – original draft.

## Declaration of competing interest

The authors declare that they have no known competing financial interests or personal relationships that could have appeared to influence the work reported in this paper.

## Acknowledgements

The authors greatly appreciate the financial support provided by the following projects:

- RETURN Extended Partnership and received funding from the European Union Next-GenerationEU, Italy (National Recovery and Resilience Plan – NRRP, Mission 4, Component 2, Investment 1.3 – D.D. 1243 2/8/2022, E0000005);
- TiSento - SENSORIALIZED COMPOSITE PIPE FOR HYDRAULIC APPLICATIONS, Italy, n. 084221000550 CUP G18I18001710007. Funded under measure 1.1.5 of the PO FESR SICILY 2014–2020;
- This research has been partially supported by the European Union - NextGenerationEU - National Sustainable Mobility Center CN00000023, Italian Ministry of University and Research Decree n. 1033— 17/06/2022, Spoke 3, CUP B73C22000760001
- SiciliAn MicronanOTecH Research And Innovation CEnter, Italy “SAMOTHRACE” (MUR, PNRR-M4C2, ECS-00000022), spoke 3 - Università degli Studi di Enna “S2-COMMs - Micro and Nanotechnologies for Smart & Sustainable Communities”.

  Anonymous referees and the Editor are acknowledged for valuable comments during the review process.

## Data availability

Data will be made available on request.

## References

Ahmed, F., Kamel, A., Abdel Jawad, S., 1996. Experimental determination of the optimal location and contraction of sedimentation tank baffles. Water Air Soil Pollut. 92 (3–4), 251–271.

Al-Sammarraee, M., Chan, A., Salim, S., Mahabaleswar, U., 2009. Large-eddy simulations of particle sedimentation in a longitudinal sedimentation basin of a water treatment plant. Part I: Particle settling performance. Chem. Eng. J. 152 (2–3), 307–314. http://dx.doi.org/10.1016/j.cej.2009.04.062.

Asgharzadeh, H., Firoozabadi, B., Afshin, H., 2011. Experimental investigation of effects of baffle configurations on the performance of a secondary sedimentation tank. Sci. Iranica 18 (4), 938–949.

Bretscher, U., Krebs, P., Hager, W.H., 1992. Improvement of flow in final settling tanks. J. Environ. Eng. 118 (3), 307–321.

Bruno, F., Bruno, P., De Marchis, M., Di Bella, G., 2024a. CFD analysis on the effect of baffles geometry on sedimentation efficiency. Lect. Notes Civ. Eng. 524 LNCE, 424–429. http://dx.doi.org/10.1007/978-3-031-63353-9_72.

Bruno, F., De Marchis, M., Napoli, E., 2024b. The role of the areal parameters on turbulent flow over 2D Gaussian roughness. Int. J. Heat Fluid Flow 106, 109287. http://dx.doi.org/10.1016/j.ijheatfluidflow.2024.109287.

Bruno, P., Di Bella, G., De Marchis, M., 2020. Perforated baffles for the optimization of disinfection treatment. Water 12 (12), 1–14.

Bruno, P., Di Bella, G., De Marchis, M., 2021. Effect of the contact tank geometry on disinfection efficiency. J. Water Process Eng. 41, 102035.

de Marchis, M., Ciraolo, G., Nasello, C., Napoli, E., 2012. Wind- and tide-induced currents in the stagnone lagoon (Sicily). Environ. Fluid Mech. 12 (1), 81–100. http://dx.doi.org/10.1007/s10652-011-9225-0.

De Marchis, M., Milici, B., 2016. Turbulence modulation by micro-particles in smooth and rough channels. Phys. Fluids 28 (11), 115101. http://dx.doi.org/10.1063/1.4966647.

De Marchis, M., Milici, B., Napoli, E., 2017. Solid sediment transport in turbulent channel flow over irregular rough boundaries. Int. J. Heat Fluid Flow 65, 114–126. http://dx.doi.org/10.1016/j.ijheatfluidflow.2017.04.006.

De Marchis, M., Milici, B., Napoli, E., 2019. Large eddy simulations on the effect of the irregular roughness shape on turbulent channel flows. Int. J. Heat Fluid Flow 80, 108494. http://dx.doi.org/10.1016/j.ijheatfluidflow.2019.108494.

De Marchis, M., Napoli, E., 2008. The effect of geometrical parameters on the discharge capacity of meandering compound channels. Adv. Water Resour. 31 (12), 1662–1673. http://dx.doi.org/10.1016/j.advwatres.2008.07.014.

Demirel, E., Aral, M.M., 2016. Unified analysis of multi-chamber contact tanks and mixing efficiency based on vorticity field. Part I: Hydrodynamic analysis. Water 8 (11), 495.

Donzis, D., Aditya, K., Sreenivasan, K., Yeung, P., 2014. The turbulent Schmidt number. J. Fluids Eng. 136, 061210. http://dx.doi.org/10.1115/1.4026619.

Fraga, B., 2017. Instantaneous transport of a passive scalar in a turbulent separated flow. Environ. Fluid Mech..

Gao, H., Stenstrom, M., 2019. Generalizing the effects of the baffling structures on the buoyancy-induced turbulence in secondary settling tanks with eleven different geometries using CFD models. Chem. Eng. Res. Des. 143, 215–225. http://dx.doi.org/10.1016/j.cherd.2019.01.015.

Goula, A.M., Kostoglou, M., Karapantsios, T.D., Zouboulis, A.I., 2008. A CFD methodology for the design of sedimentation tanks in potable water treatment: Case study: The influence of a feed flow control baffle. Chem. Eng. J. 140 (1–3), 110–121.

Huggins, D.L., Piedrahita, R.H., Rumsey, T., 2004. Analysis of sediment transport modeling using computational fluid dynamics (CFD) for aquaculture raceways. Aquac. Eng. 31 (3–4), 277–293.

Imam, E., McCorquodale, J.A., Bewtra, J., 1983. Numerical modeling of sedimentation tanks. J. Hydraul. Eng. 109 (12), 1740–1754.

Kim, D., Kim, D.-I., Kim, J.-H., Stoesser, T., 2010. Large eddy simulation of flow and tracer transport in multichamber ozone contactors. J. Environ. Eng. 136 (1), 22–31.

Krebs, P., Vischer, D., Gujer, W., 1995. Inlet-structure design for final clarifiers. J. Environ. Eng. 121 (8), 558–564.

Li, H., Balachandar, S., Sansalone, J., 2021a. Large-eddy simulation of flow turbulence in clarification systems. Acta Mech. 232 (4), 1389–1412. http://dx.doi.org/10.1007/s00707-020-02914-1.

Li, H., Sansalone, J., 2020. Cfd as a complementary tool to benchmark physical testing of pm separation by unit operations. J. Environ. Eng. (U. S.) 146 (11), http://dx.doi.org/10.1061/(ASCE)EE.1943-7870.0001803.

Li, H., Sansalone, J., 2021a. Benchmarking Reynolds-averaged Navier-Stokes turbulence models for water clarification systems. J. Environ. Eng. (U. S.) 147 (9), http://dx.doi.org/10.1061/(ASCE)EE.1943-7870.0001889.

Li, H., Sansalone, J., 2021b. CFD with evolutionary optimization for stormwater basin retrofits. J. Environ. Eng. (U. S.) 147 (7), http://dx.doi.org/10.1061/(ASCE)EE.1943-7870.0001881.

Li, H., Sansalone, J., 2022a. A CFD-ML augmented alternative to residence time for clarification basin scaling and design. Water Res. 209, http://dx.doi.org/10.1016/j.watres.2021.117965, All Open Access, Bronze Open Access.

Li, H., Sansalone, J., 2022b. Implementing machine learning to optimize the cost-benefit of urban water clarifier geometrics. Water Res. 220, http://dx.doi.org/10.1016/j.watres.2022.118685.

Li, H., Sansalone, J., 2022c. InterAdsFoam: An open-source CFD model for granular media-adsorption systems with dynamic reaction zones subject to uncontrolled urban water fluxes. J. Environ. Eng. (U. S.) 148 (9), http://dx.doi.org/10.1061/(ASCE)EE.1943-7870.0002027.

Li, H., Spelman, D., Sansalone, J., 2021b. Baffled clarification basin hydrodynamics and elution in a continuous time domain. J. Hydrol. 595, http://dx.doi.org/10.1016/j.jhydrol.2021.125958, All Open Access, Bronze Open Access.

Li, H., Spelman, D., Sansalone, J., 2024. Unit operation and process modeling with physics-informed machine learning. J. Environ. Eng. (U. S.) 150 (4), http://dx.doi.org/10.1061/JOEEDU.EEENG-7467, All Open Access, Hybrid Gold Open Access.

Milici, B., De Marchis, M., 2016. Statistics of inertial particle deviation from fluid particle trajectories in horizontal rough wall turbulent channel flow. Int. J. Heat Fluid Flow 60, 1–11. http://dx.doi.org/10.1016/j.ijheatfluidflow.2016.03.008.

Milici, B., De Marchis, M., Napoli, E., 2020. Large eddy simulation of inertial particles dispersion in a turbulent gas-particle channel flow bounded by rough walls. Acta Mech. 231 (9), 3925–3946. http://dx.doi.org/10.1007/s00707-020-02740-5.

Razmi, A., Firouzabadi, B., Ahmadi, G., 2009. Experimental and numerical approach to enlargement of performance of primary settling tanks. J. Appl. Fluid Mech..

Rostami, F., Shahrokhi, M., Said, M.A.M., Abdullah, R., et al., 2011. Numerical modeling on inlet aperture effects on flow pattern in primary settling tanks. Appl. Math. Model. 35 (6), 3012–3020.

Saccone, D., De Marchis, M., Milici, B., Marchioli, C., 2023. Transport of inertial ellipsoidal particles in turbulent flow over rough walls. Phys. Rev. Fluids 8 (8), http://dx.doi.org/10.1103/PhysRevFluids.8.084303.

Samstag, R., Ducoste, J., Griborio, A., Nopens, I., Batstone, D., Wicks, J., Saunders, S., Wicklein, E., Kenny, G., Laurent, J., 2016. CFD for wastewater treatment: An overview. Water Sci. Technol. 74 (3), 549–563. http://dx.doi.org/10.2166/wst.2016.249.

Shahrokhi, M., Rostami, F., Said, M.A.M., Yazdi, S.R.S., et al., 2012. The effect of number of baffles on the improvement efficiency of primary sedimentation tanks. Appl. Math. Model. 36 (8), 3725–3735.

Shahrokhi, M., Rostami, F., Said, M.A.M., et al., 2013. Numerical modeling of baffle location effects on the flow pattern of primary sedimentation tanks. Appl. Math. Model. 37 (6), 4486–4496.

Su, J., Wang, L., Zhang, Y., Gu, Z., 2019. A numerical study on influent flow rate variations in a secondary settling tank. Processes 7 (12), http://dx.doi.org/10.3390/PR7120884.

Tamayol, A., Firoozabadi, B., Ahmadi, G., 2008. Effects of inlet position and baffle configuration on hydraulic performance of primary settling tanks. J. Hydraul. Eng. 134 (7), 1004–1009. http://dx.doi.org/10.1061/(ASCE)0733-9429(2008)134:7(1004).

Tamayol, A., Firoozabadi, B., Ashjari, M., 2010. Hydrodynamics of secondary settling tanks and increasing their performance using baffles. J. Environ. Eng. 136 (1), 32–39. http://dx.doi.org/10.1061/(ASCE)EE.1943-7870.0000126.

Wills, R., Davis, C., 1964. Flow patterns in a rectangular sewage sedimentation tank. In: Advances in Water Pollution Research. Elsevier, pp. 335–385.

Zhang, J., Tejada-Martínez, A., Zhang, Q., 2013. Reynolds-averaged Navier-Stokes simulation of the flow and tracer transport in a multichambered ozone contactor. J. Environ. Eng. 139 (3), 450–454.

Zhang, J., Tejada-Martínez, A.E., Zhang, Q., 2014. Developments in computational fluid dynamics-based modeling for disinfection technologies over the last two decades: A review. Environ. Model. Softw. 58, 71–85.

Zhou, S., McCorquodale, J.A., Vitasovic, Z., 1992. Influences of density on circular clarifiers with baffles. J. Environ. Eng. 118 (6), 829–847.